Seismic hazard assessment
for the Tbilisi test area (eastern Georgia)

D. Slejko[1], Z. Javakhishvili[2], A. Rebez[1], M. Santulin[1], M. Elashvili[2], P.L. Bragato[1], T. Godoladze[2] and J. Garcia[3]

[1] Istituto Nazionale di Oceanografia e di Geofisica Sperimentale, Trieste-Udine, Italy
[2] Seismic Monitoring Center, Tbilisi, Georgia
[3] Centro Nacional de Investigaciones Sismológicas, La Habana, Cuba

ABSTRACT The seismic hazard of eastern Georgia has been computed with the seismotectonic probabilism approach. A logic tree was used to take into account the different hypotheses on the seismogenesis of the Caucasus region, and to model seismicity and attenuation. In addition to the usual maps referring to different types of terrains (rock, stiff, and soft soil), the soil hazard map for the Tbilisi broader area has been computed by aggregating the results according to the specific characteristics of the terrains. Ground motions between 0.16 and 0.32 g are expected in accordance with the soil conditions in Tbilisi town, while values between 0.32 and 0.40 are expected towards the Caucasus ridge. The uniform hazard response spectrum for Tbilisi for rock and stiff soil is almost flat for periods lower than 0.3 s. This decreases for higher periods, while the decrease is less evident for soft soil and the spectrum remains high for periods lower than 0.5 s.

1. Introduction

The Caucasus is located between the Black and the Caspian Seas and belongs presently to Russia, Georgia, Armenia, and Azerbaijan. It is a part of the Alpine – Himalayan collision belt and it is well known for its high seismicity. Strong earthquakes with magnitude larger than 6.5 occurred also recently causing deaths and widespread damage. The 1988 Spitak earthquake with magnitude 7.2, the 1991 Racha earthquake with magnitude 7.3, and the 1992 Barisakho - Kazbegi earthquake with magnitude 6.8 are all worth mentioning. Although the geodynamic activity of the region, caused by the convergence of the Arabian and the Eurasian plates at a rate of several cm/year, is well known, different tectonic models were proposed as an explanation for the seismic process in the region (Philip *et al.,* 1989; Jackson, 1992; Triep *et al.,* 1995).

The Caucasus region was one of the test areas of the Global Seismic Hazard Assessment Project (GSHAP) developed between 1993 and 1999 which aimed at constructing the global seismic hazard map of our planet (Giardini and Basham, 1993; Giardini, 1999). In the framework of GSHAP, four different teams participated in the seismic hazard assessment of the Caucasus (Balassanian *et al.,* 1999) and some interesting results were obtained although it was not possible to converge to a final hazard map but several maps were constructed (e.g.: Martirosyan *et al.,* 1999). More precisely, two different seismogenic zonations were used in the hazard computations: one was a lineament model, and the second was a lineament-domain-focal model.

On those bases, six hazard maps were obtained with different approaches: 1) seismotectonic-probabilistic; 2) deterministic-probabilistic; 3) aerial probabilistic; 4) deterministic; 5) probabilistic; and 6) historical-probabilistic.

In July 2004, the SETA (SEismic hazard assessment for the Tbilisi test Area) project was launched: it was a co-operation project supported by the Italian Government through the Italian law 212/92 of a duration of 2 years. The main aims of the SETA project were the installation of a regional seismometric network, the identification of the active faults in the region by SAR and optical image analysis, the construction of a DEM for the Tbilisi test area, the computation of the soil seismic hazard map for the Tbilisi broader area, and the technological transfer and training of Georgian scientists. Two areas have been considered for the seismic hazard assessment: eastern Georgia, which is about 60,000 km^2 wide around Tbilisi, and the broader Tbilisi area, which is about 6,000 km^2 wide around the town (see Fig. 1). The influence of the earthquakes that occurred in a larger region (an area with a 200-km ray centred in Tbilisi town) was considered in both cases. Also the site effects were modelled at a large scale for the Tbilisi broader area and the soil seismic hazard map was produced.

The aim of the present paper is to make a report on the study undertaken for the computation of the seismic hazard maps of eastern Georgia and for the soil seismic hazard map of the Tbilisi broader area, highlighting the operations used to characterize the uncertainties associated with any seismic hazard assessment.

2. Characteristics of the PSHA

Two approaches can be followed in the seismic hazard analysis: the deterministic method and the probabilistic one. The probabilistic approach is by far the one preferred for seismic zonation and for seismic hazard analysis of strategic facilities (McGuire, 2001). The probabilistic seismic hazard assessment (PSHA) of eastern Georgia and that of the Tbilisi broader region have been made according to the standard approach of Cornell (1968) by using the computer formulation of Bender and Perkins (1987). This approach is based on two working hypotheses: the earthquake recurrence times follow a Poisson distribution (made up of independent, non-multiple events, and the process is stationary in time) and the magnitude is exponentially distributed [the Gutenberg - Richter (G-R) relation holds]. In addition, the seismicity is considered uniformly distributed over the seismogenic zone (SZ). The Cornell (1968) method, then, needs the following input data: the definition of the geometry of the seismogenic sources, the characteristics of the seismicity inside the seismogenic sources [in terms of average number of earthquakes per magnitude class, and maximum possible magnitude (M_{max})], and the attenuation relation (AR) of the parameter chosen to describe the ground motion.

The quantification of the uncertainties (McGuire, 1977) is a crucial point in the modern PSHA. Two kinds of uncertainties characterise the results in PSHA: the aleatory variability and the epistemic uncertainty (McGuire and Shedlock, 1981; Toro *et al.,* 1997). Aleatory variability is the natural randomness in a process. It is considered in the PSHA when taking into account the standard deviation of the relation describing the process. The epistemic uncertainty is the scientific uncertainty in the model of the process and it is due to limited data and knowledge.
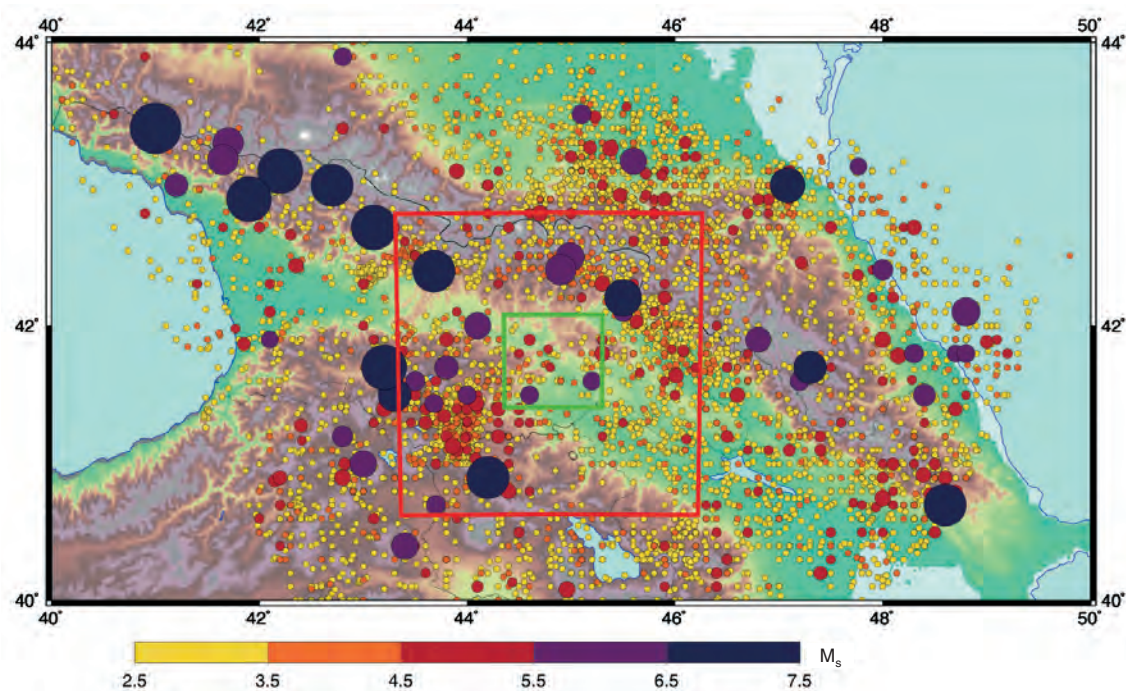
Fig. 1 - Epicentres of the earthquakes that occurred in the Caucasus from 453 to 2003. Only 2 events are reported in the catalogue before year 1000, and a further 12 before 1800. The large square indicates eastern Georgia, while the small square indicates the broader Tbilisi area.

It is considered in the PSHA when using alternative models. The logic tree approach for the PSHA (Kulkarni *et al.,* 1984; Coppersmith and Youngs, 1986) has been introduced to quantify the epistemic uncertainties. Each node of the logic tree collects a series of choices, represented by each branch of the logic tree. The final aggregate result is obtained by adequately weighting the individual results coming from the different branches [see more discussion in Rebez and Slejko (2004)].

In the present study, an articulated logic tree (Fig. 2) with 10 branches has been constructed for the rock and soft soil hazard maps: it consists of two zonations (one of them has 4 different geometries) and two methods for M_{max} assessment. In the case of the stiff soil hazard map, a further AR, ad hoc developed for the study region, has been considered, bringing the branches of the logic tree to 20.

Most of the efforts were devoted to the representation of the regional seismogenesis, in fact a good knowledge of the geometry and seismicity of the seismogenic sources in the study region is requested for a modern PSHA. When the seismogenic model is not universally accepted, different hypotheses can be considered and mixed together in the hazard calculation by means of the logic tree approach. The other basic element for a PSHA is the earthquake catalogue, whose events contribute to the spatial definition of the seismogenic sources and characterize them from the seismicity point of view.
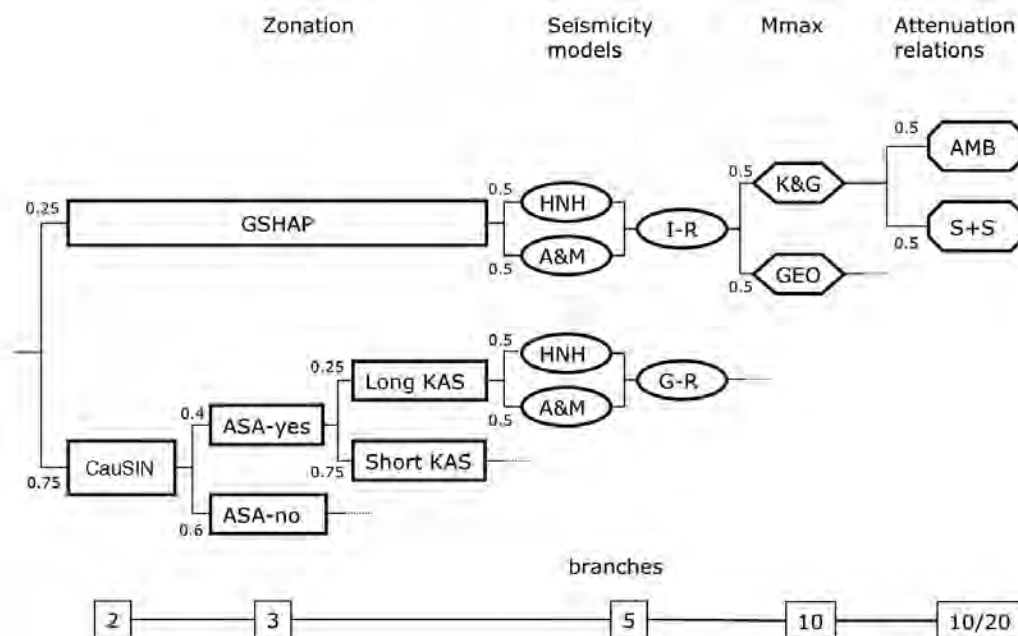
Fig. 2 - The logic tree of the SETA project. It consists of 10 branches: 2 main seismogenic zonations (for one of them 4 different alternatives are considered), 2 methods for assessing the seismicity rates, which are then averaged, 2 approaches for computing M_{max}, and 1 *PGA* attenuation relation (AMB) for rock and soft soil. In the case of stiff soil a second attenuation (S+S) relation was used, leading the number of branches to 20. The numbers indicate the weights associated with the different branches.

3. The earthquake catalogue

The data base for PSHA is the earthquake catalogue. All the main historical events of the catalogue prepared during the GSHAP project (Balassanian *et al.,* 1999), which occurred within a 200 km distance from Tbilisi town, were revised on the basis of the available literature (Bius, 1948, 1952, 1955; Kondorskaya and Shebalin, 1982; Shebalin and Tatevossian, 1997; Varazanashvili and Papalasvili, 1998) and through the documents found by a specific research in the Georgian archives. Special investigations were carried out for some selected strong earthquakes which occurred in the vicinity of Tbilisi. More precisely, the data available in the state library about the main events of the 19th and the beginning of the 20th century were studied. Special attention was paid to the 1896 earthquake, which is considered the largest in the territory under investigation, with a magnitude around 6 and with the strongest effects (intensity VII MSK) in Tbilisi. The main improvements refer to the epicenter locations while no modifications were introduced to the magnitudes taken from the GSHAP catalogue (Balassanian *et al.,* 1999), where the surface wave magnitude (M_S) was obtained from intensity according to the Kondorskaya and Shebalin (1982) procedure. The M_S of the small events of the 20th century was computed by a proper conversion (Rautian *et al.,* 2007) of the energy class originally calculated from the recordings.

In parallel, also the instrumental seismicity was revised. The instrumental period in the Caucasus began in 1899 when the seismological station of Tbilisi was installed. At the beginning
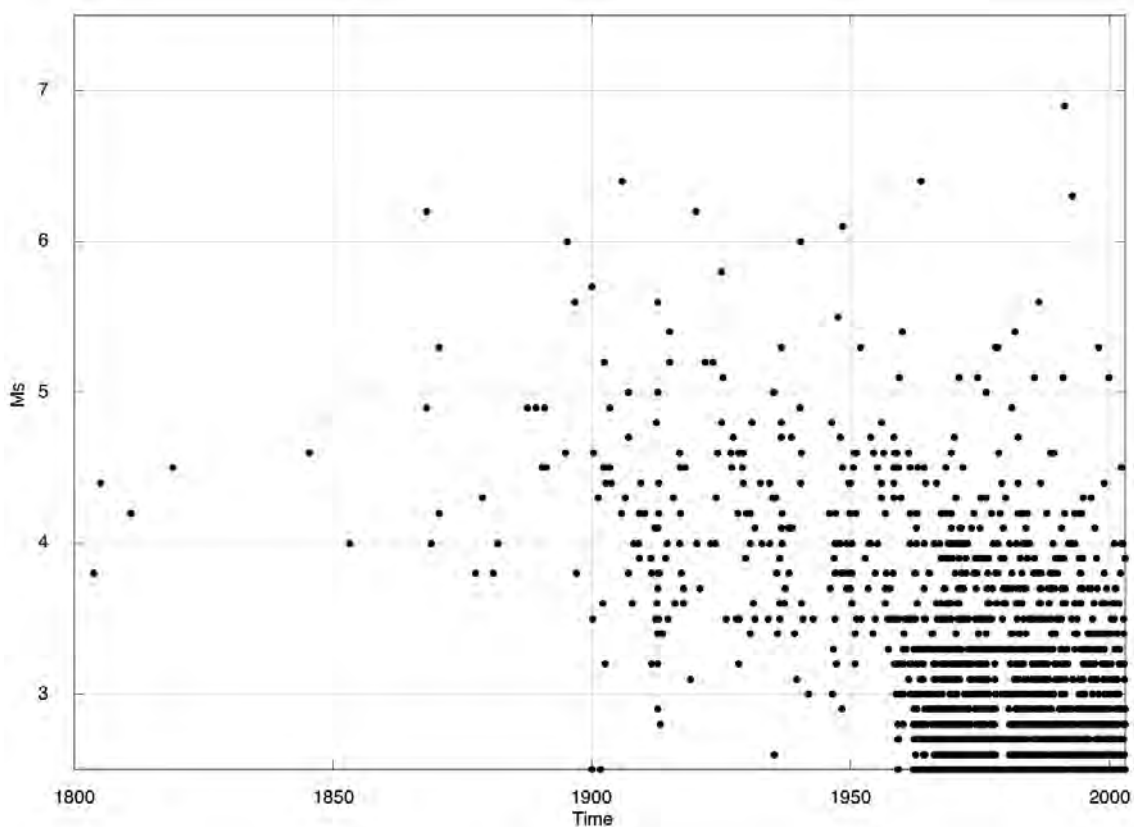
Fig. 3 - Time distribution of the event magnitude in the adopted earthquake catalogue. The events before 1800 are not shown because they are very rare: only 2 events, in fact, are reported in the catalogue before year 1000, and further 12 before 1800.

of the 20th century some additional seismic stations were set up: they were equipped with low sensitivity instruments generally of mechanical type. The regional system of seismological data acquisition and treatment for Georgia was established in 1950 but the modern instrumental period for the Caucasus started only in 1962, when the network was equipped with high sensitivity seismometers and the threshold magnitude of event detection was reduced to 1.5 (Kondorskaya and Shebalin, 1982).

At the end of the specific investigations described above a new catalogue (hereafter SETA catalogue) was obtained for the PSHA of eastern Georgia and the Tbilisi broader area. It consists of 6057 events which occurred from 453 to 2003 in the Caucasus and surrounding regions (Fig. 1). The threshold magnitude is M_S 2.5 but the catalogue is very poor before 1800 and only a few earthquakes with magnitude larger than 6 are reported. Also the 19th century is rather poorly documented for all magnitudes (Fig. 3), while an improvement of the data acquisition from 1900 is evident.

The completeness of the catalogue has been evaluated for each magnitude class, according to the chosen 0.3 step, by the Stepp (1972) graphs, where the cumulative number of events of the
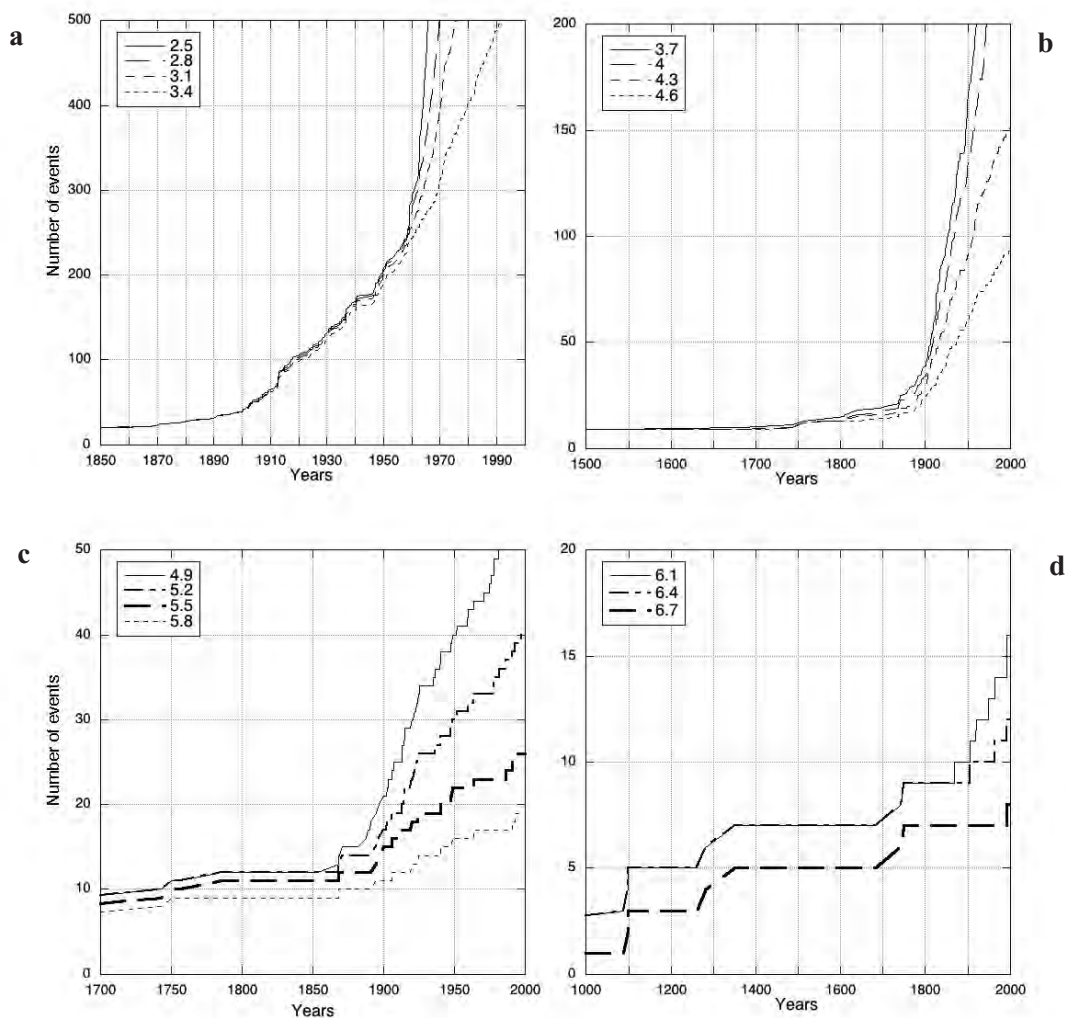
Fig. 4 - Stepp graphs for the different M_s classes: each class is 0.3 magnitude units wide. M_s range: a) 2.4-3.5; b) 3.6-4.7; c) 4.8-5.9; d) 6.0-6.8.

investigated magnitude class vs. time is represented (Fig. 4). The abrupt slope increases of the linear trend identify the dates when the catalogue starts to be richer with events, and, consequently, better documented. In this way, the completeness of the catalogue for the different magnitude classes remains identified. Correctly, it should be stated that the periods identified represent periods when the seismicity is stationary in time but the stationarity of the seismic process is a working hypothesis in the PSHA and, consequently, stationarity and completeness can be considered equivalent. Fig. 5 reports the results of the analysis of completeness. It can be seen that a long period refers only to large magnitude classes (6.7 and larger) and the completeness of almost all the other classes is limited to periods of the last two centuries.

The space distribution of the earthquake epicentres displayed in Fig. 1 clearly shows that the
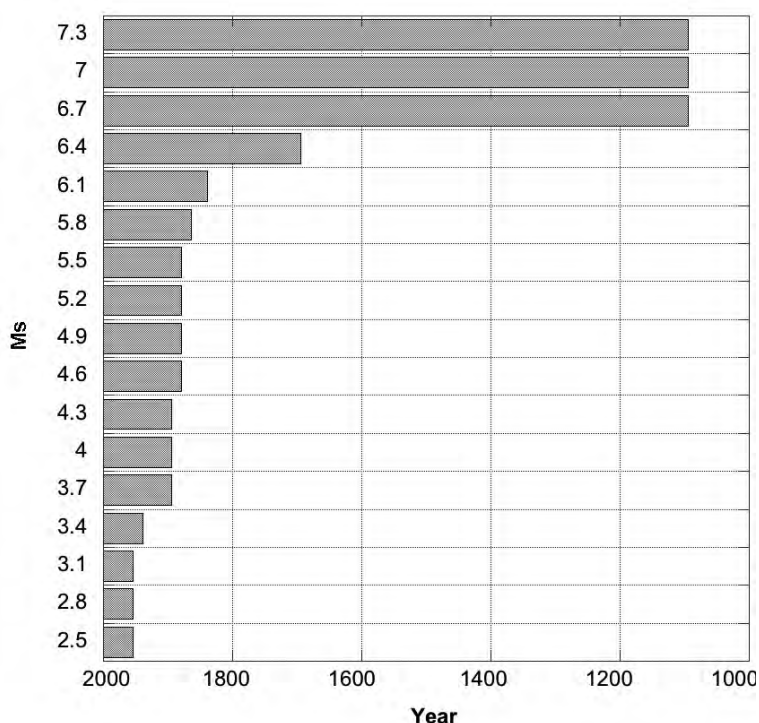
Fig. 5 - Completeness periods for the different M_s classes. The value reported on the *y*-axis is the central value of the class, which is 0.3 magnitude units wide. It can be seen that the completeness for very large earthquakes only is longer than the last 200 years.

central strip of Georgia, where the town of Tbilisi is also located, is relatively quiet while several strong events occurred east and north of the town at a distance larger than 100 km.

4. SZ geometry

The GSHAP project has brought together the different, existing ideas about seismogenesis in the Caucasus. To take into proper account all the different hypotheses, it was decided to consider alternative seismogenic zonation in the logic tree structure. In the standard PSHA, seismic sources are modelled as lines representing the surficial projection of faults or as wide areas (SZs), where the earthquakes can occur randomly. Two basic seismogenic zonations have been considered for the present PSHA: they represent different levels of seismotectonic knowledge. The first seismogenic zonation derives directly from the main one used in the GSHAP and it consists of faults which are mainly WNW-ESE oriented, in agreement with the main trend of the Caucasus mountain chain. The second seismogenic zonation represents the most recent model on seismogenic sources available for the Caucasus and derives from recent seismotectonic studies performed in Georgia in the framework of an international project called CauSIN (http://CauSIN.org). In this second zonation, some alternative hypotheses of fault activations were planned (Fig. 2): they refer to the importance that can be given to some large faults normal to the regional WNW-ESE trend of the Caucasus chain.

Entering into detail, in the case of the GSHAP zonation (Fig. 6), a buffer zone around the
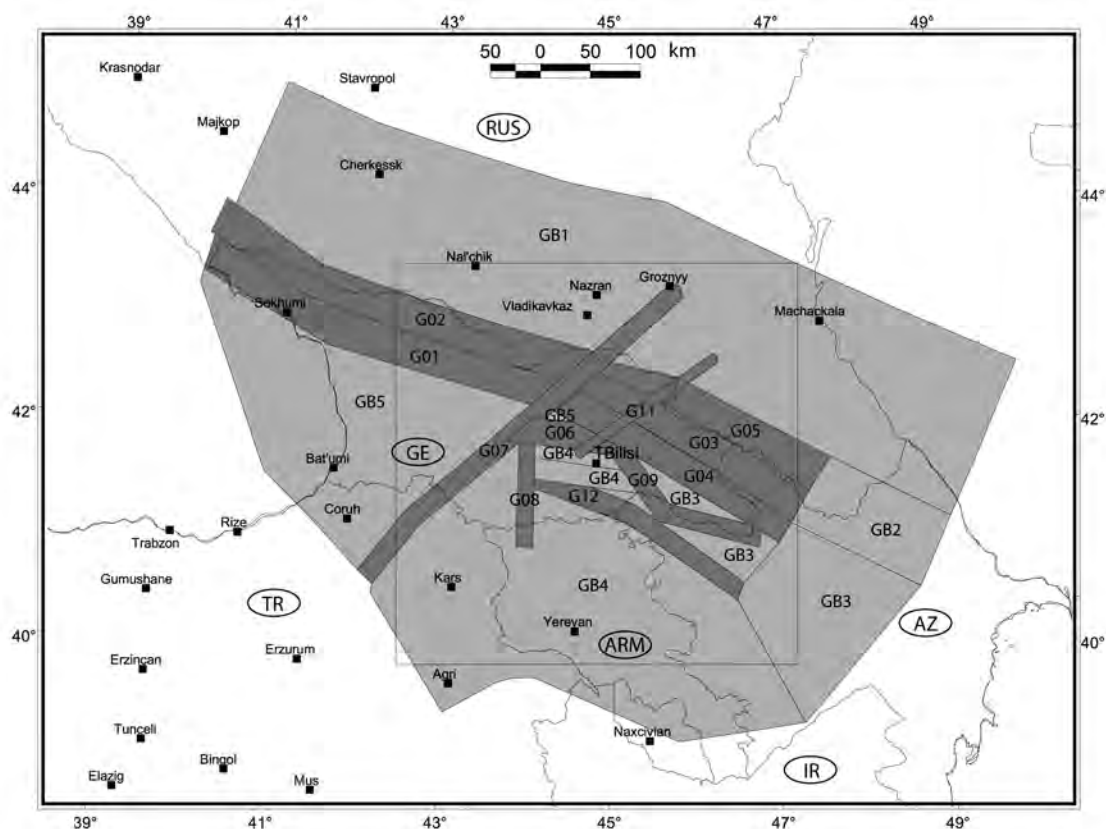
Fig. 6 - The GSHAP zonation (modified from Balassanian *et al.,* 1999). It consists of 12 SZs (G01 to G12) and 5 background zones (GB1 to GB5). The background SZs GB3 and GB4 are formed by 3 separate parts. The background SZ GB5 is formed by 2 separate parts.

faults of that zonation was considered and, consequently, faults have been substituted with SZs. This modification from the original zonation was motivated by the fact that different geometries for some faults were proposed and used in GSHAP, suggesting that an ultimate model was not available at that time. A model based on SZs seems, then, more suitable to capture those uncertainties and, moreover, it is an alternative to the CauSIN zonation, which is based on faults.

The CauSIN zonation (Fig. 7) considers 11 faults (zones C01 to C11) and 5 SZs (zones C12 to C16). Alternative hypotheses have been considered for two major faults: the Borjomi – Kazbegi and the Asa – Aragvi faults. As different opinions exist about the present activity of the Asa – Aragvi fault (zone C11), both possibilities have been considered: 1) the Asa – Aragvi fault is an active fault ("ASA-yes" branch in the logic tree of Fig. 2) and 2) it is not an active fault and, consequently, it is not considered ("ASA-no" branch in the logic tree of Fig. 2). Different opinions about the activity of the Borjomi – Kazbegi fault [zone C02; Gamkrelidze *et al.* (1998)] also exist: it is considered active along its whole length (red plus green lines in Fig. 7 corresponding to the "Long KAS" branch in the logic tree of Fig. 2) or along only the Tskhinvali – Kazbegi sector (red line only in Fig. 7 corresponding to the "Short KAS" branch in the logic tree of Fig. 2).
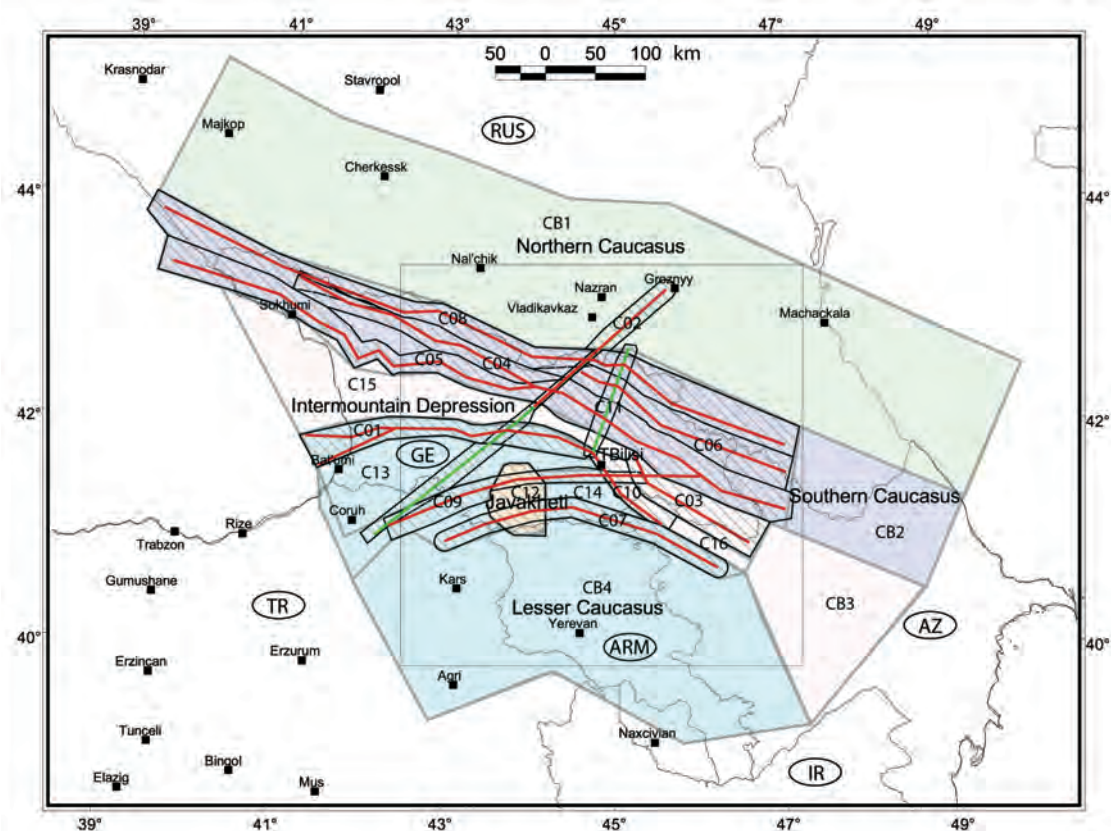
Fig. 7 - The CauSIN zonation summarizes 4 slightly different zonations where: 1) either the total length of the Kazbegi fault is considered active or only the northern sector; and 2) the Asa - Aragvi fault is considered either active or not. The zonation consists of 11 faults (zones C1 to C11), 4 SZs (zones C12 to C15), and 4 background zones (CB1 to CB4). The coloured areas indicate the macro-zones used for the *b*-value calculation. The dashed area shows the area interested by the active faults (red lines) and probable active faults (green lines).

In addition to the seismogenic sources previously described, some background zones have been defined: 5 for the GSHAP zonation (zones GB1 to GB5 in Fig. 6) and 4 for the CauSIN zonation (zones CB1 to CB4 in Fig. 7). They collect the diffuse seismicity which is not possible to associate to any of the major tectonic elements (faults and SZs) of the two zonations.

In the logic tree approach, each branch must be properly weighted and the sum at each node must be 1. A remarkable preference was given to the CauSIN zonation (weight 0.75) with respect to the GSHAP one. The fossil character of the Asa – Aragvi fault ("ASA-no" branch in Fig. 2) was preferred (weight 0.6) and the activity of only the Tskhinvali – Kazbegi sector ("Short KAS" branch in Fig. 2) of the Borjomi – Kazbegi fault was considered much more probable (weight 0.75).

5. Seismicity rates

The association of earthquakes to faults in the CauSIN zonation has been done considering a

variable buffer (width is about 10 to 15 km based on the regional tectonic setting and the total width of the active faults belonging to the different systems) around the fault. Where faults intersect, the association of the earthquakes to one of the two was based on an expert opinion. In general, the number of events of the individual fault was rather low and considered not suitable for a robust estimate of the seismicity parameters. As countermeasure, 4 seismotectonic macro-zones, collecting more faults of similar seismotectonic behaviour, were introduced: Northern Caucasus, Southern Caucasus, Intermountain Depression, and Minor Caucasus (Fig. 7). The Javakheti SZ (C11 in Fig. 7) was rich enough of events and its immersion in a wider zone was not needed.

The seismicity rates (annual number of earthquakes of magnitude between M_S-0.1 and M_S+0.1, where M_S is the reference magnitude of the class, because the class is 0.3 wide) of the seismogenic sources have been computed according to two statistical approaches: the "higher not highest" (HNH) method (Slejko *et al.,* 1998), already used in preparing the seismic hazard map of the Italian territory (Slejko *et al.,* 1998), and the Albarello and Mucciarelli (2002: A&M) method, already used for the updated version of the Italian seismic hazard map (Albarello *et al.,* 2000). The rates computed for each magnitude class, in the two different methods, were not applied directly but were averaged with equal weight. In this case, the number of branches of the logic tree does not increase: this is a sort of trimming of the logic tree to avoid useless computation because it was demonstrated (Barani *et al.,* 2007) that the influence of these two different approaches is marginal in the final results. The individual, average rates were used for the GSHAP zonation directly (I-R branch in the logic tree of Fig. 2), while the cumulative rates were fitted to the G-R relation for the CauSIN zonation and the individual rates were then computed (G-R branch in the logic tree of Fig. 2). More precisely, the *b*-value of the G-R relation was calculated for the 4 seismotectonic macro-zones and for the Javakheti SZ and it was kept fixed for all the faults inside each macro-zone. Given the *b*-value, the *a*-value was computed individually for each fault on the basis of the earthquakes associated to that specific fault.

6. M_{max}

The M_{max} for each seismogenic source (fault or SZ), to be introduced into the PSHA, was estimated in two different ways: the first was statistical while the second was based on geological information.

The statistical method [Kjiko and Graham (1998): K&G] computes M_{max} and the related uncertainty for a source using as input data: the maximum observed magnitude, the threshold magnitude considered complete in the catalogue, the average error in the magnitude estimates (fixed in our case arbitrarily at 0.2), the *b*-value of the G-R relation and its standard deviation, the annual rate (i.e.: the number of earthquakes with magnitude greater than, or equal to, the threshold magnitude) and the catalogue time span which is considered complete. This last parameter was set at 300 years (which can be considered the documented period of the catalogue for high magnitudes) as both methodologies used for the seismicity rate computation scan the whole catalogue and either choose the period which is most seismic in agreement with the return period of each magnitude class, a priori estimated (HNH method), or average the weighted seismicity rates computed on different periods (A&M method). The K&G approach considers

four formulations for the M_{max} computation: the most robust Bayesian Kijko-Sellevol formula was applied here. It was possible to compute an M_{max} different from the maximum observed one only for some SZs and also in these cases the increment was limited (in general 0.1), which depended on the rather long completeness period (300 years) considered.

The second method is a geological (GEO) approach and it is based on the tectonic characteristics of each source. More precisely, the sources were segmented, each segment representing a single structure where the rupture may propagate. The segmentation was done according to the tectonic setting and was based on an expert opinion (Gamkrelidze, personal communication).

No univocal definition is available for the fault rupture length: the general use is to take the half of the total length (Mark, 1977) but also the lower value of one third was often used. We took the one third of the total fault length as rupture length. It was, then, possible to compute M_{max} according to the relations calibrated by Wells and Coppersmith (1994).

In the case of the background zones of both zonations, where it is not reasonable to define the longest fault, the "one step beyond" (1SB) method (Slejko et al., 1998) was used. This approach, which was already used for the Italian seismic hazard map (Slejko et al., 1998), extrapolates the observed seismicity rates by one step (in the present study 0.3 magnitude units) according to the G-R b-value of the SZ when the corresponding return period exceeds the time length of the earthquake catalogue [1000 years because the catalogue reports the very strong earthquakes of the last millenium; see more detailed description in Slejko et al. (1998)]. For some background zones, it was not possible to define a maximum magnitude according to the 1SB method because the maximum magnitude computed for them refers to a return period shorter than 1000 years and the events should, then, be contained in the catalogue.

The seismicity rate related to M_{max} was computed extrapolating the G-R interpolation of the cumulative seismicity rates, whatever the method used to apply them (I-R or G-R). M_{max} was applied in different ways to the PSHA: by adding all the rates (calculated through the G-R relation) from the maximum observed magnitude to the K&G M_{max}, or by adding only the rate of the GEO or 1SB M_{max}.

As we had no solid reasons to prefer one of the two approaches, equal weight was given to them in the logic tree (see Fig. 2).

7. Attenuation

Two ARs for horizontal peak ground acceleration (*PGA*) were used for the PSHA: the first was calibrated on European earthquakes (Ambraseys et al., 1996: AMB), the second is a mixture between an ad hoc relation developed in the SETA project and that for Caucasian earthquakes proposed by Smit et al. (2000).

The SETA relation was calibrated on data of the European strong motion data bank (Ambraseys et al., 2000, 2004) related to earthquakes that occurred in the Caucasus (36°-46° N, 38°-52° E). As M_S was not available for all the events, all the other magnitudes (M_L, M_W, m_b) were transformed into M_S using the relations by Camassi and Stucchi (1997), Gruppo di Lavoro (2004), and Ambraseys (1990) for M_L, M_W and m_b, respectively. Two hundred *PGA* values referring to earthquakes with an M_S larger than, or equal, to 4.0 and an epicentral distance shorter
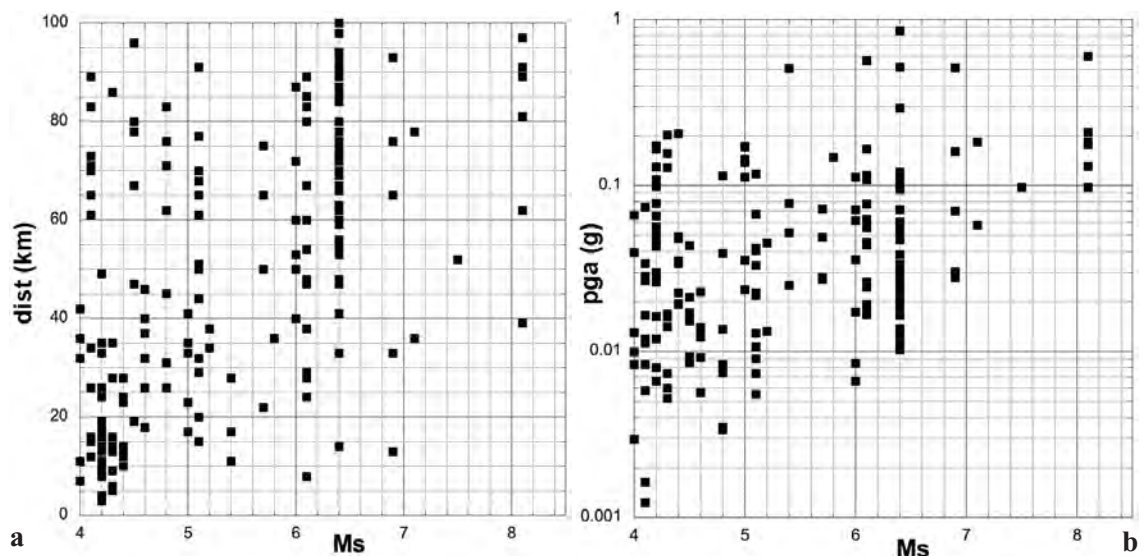
Fig. 8 – Data used for the SETA attenuation relation: a) distance vs. M_S, b) *PGA* vs. M_S.

than 100 km were considered suitable for the regression because data referring to greater distances are available only for high magnitude events. Fig. 8 shows the contents of the data set used: only 8 *PGAs* are lower than 0.005 g (Fig. 8b), which is considered the trigger level of the instruments. The attenuation model used has the functional form (Bragato and Slejko, 2005):

$$\log_{10}PGA = a + (b+cM_S)\, M_S + (d+eM_S)\, \log_{10}r \qquad \text{with } r^2 = D^2 + h^2 \qquad (1)$$

where *PGA* is expressed in g, *D* is the epicentral distance, while *a, b, c, d, e* and *h* are parameters estimated by regression on the available data set. In the estimation, the bias induced by non-triggering stations was taken into account and the techniques for Truncated Regression Analysis described by Bragato (2004) was adopted.

The following relation was obtained:

$$\log_{10}PGA = -2.14 + (0.98-0.06M_S)\, M_S + (-1.88+0.0009M_S)\, \log_{10}r \qquad (2)$$

with *h* = 13.4 and standard deviation=0.35.

This relation is considered valid for an epicentral distance shorter than 100 km.

As in the PSHA also distant earthquakes can contribute towards constructing the expected ground motion at the studied site, it was necessary to improve the SETA relation for further distances. It was decided to use the Smit *et al.* (2000) relation for this scope as it was calibrated on almost the same data set but considering a different attenuation model. This combined relation is indicated as S+S hereafter and in the logic tree of Fig. 2. We took as its standard deviation the mean of the SETA and Smit *et al.* (2000) ARs.
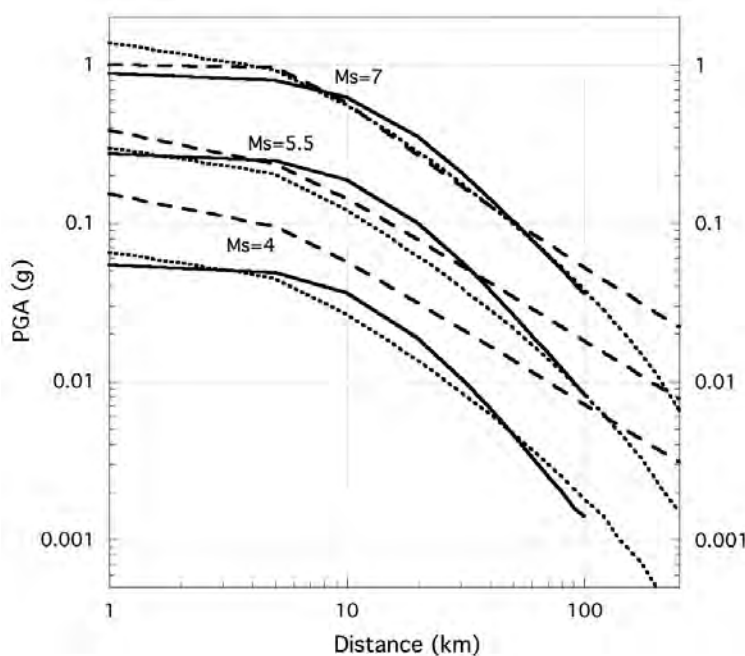
Fig. 9 - Three *PGA* attenuation relations for the Caucasus referring to M_S 4, 5.5, and 7: SETA (solid line), AMB (dashed line), Smit *et al.* (2000) (dotted line).

The AMB relation was defined for three soil types: rock, stiff, and soft soils while the S+S relation can be considered adequate for stiff soil only, according to the data used for its calibration. A comparison between the SETA and the AMB (stiff soil) ARs is proposed in Fig. 9: for all magnitudes the AMB relation forecasts higher ground motions in the far field and the expected *PGAs* are much higher for all distances in the case of low magnitudes. For an additional comparison, the original Smit *et al.* (2000) AR is also reported in Fig. 9: it differs mainly for low and medium magnitudes in the medium field (distances from 5 to 50 km), where it forecasts lower ground motions.

The AMB AR has the advantage of being calibrated on a very large data set, while the S+S relation has the advantage of modelling regional earthquakes. Consequently, equal weight was given to them in the logic tree (see Fig. 2).

8. The seismic hazard maps of eastern Georgia

The PSHA of eastern Georgia was performed in terms of *PGA* according to the Cornell (1968) approach in the Bender and Perkins (1987) formulation. The hazard estimates refer to a 475-year return period, corresponding to the 10% exceedence probability in 50 years, standard European reference in seismic design (CEN, 2002). The variability of the attenuation model has been taken into account considering the standard deviation in the hazard computation. The following hazard maps show the estimates obtained by aggregating the results coming from the individual branches of the logic tree (10 in the case of rock and soft soil, 20 in the case of stiff soil) weighted accordingly (see the weights at each node in Fig. 2): the median *PGA*, calculated considering the AR variability (standard deviation), is mapped and the epistemic uncertainty is implicitly
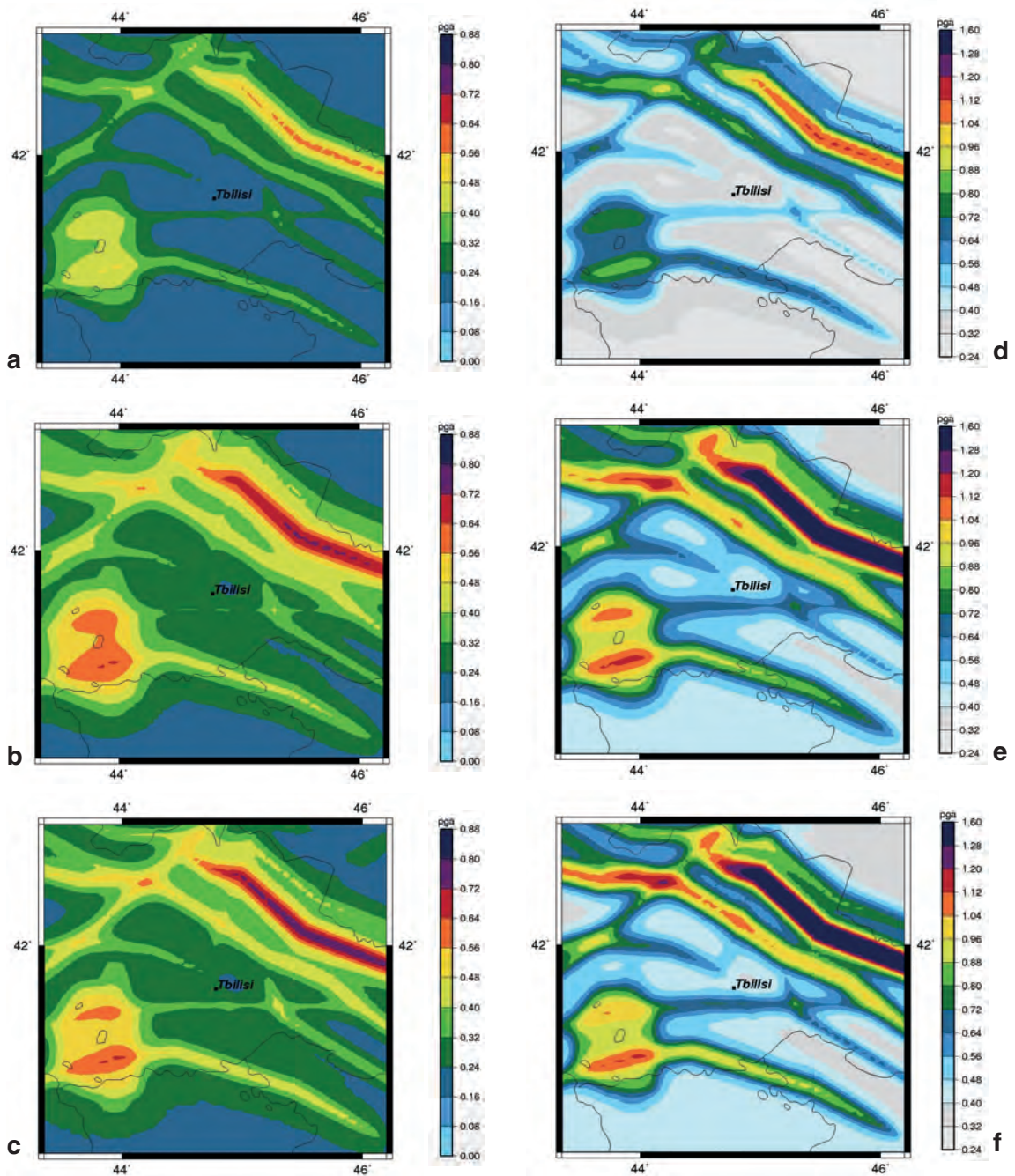
Fig. 10 – Seismic hazard of eastern Georgia in terms of *PGA* computed taking into account the attenuation variability: for a 475-year return period on rock (a), stiff soil (b), and soft soil (c); for a 2475-year return period on rock (d), stiff soil (e), and soft soil (f).

considered because the average value of the branches is taken.

Figs. 10a, 10b, and 10c collect the results obtained for the 3 soil types considered: rock, stiff, and soil soils. The rock hazard map (Fig. 10a) is the most interesting as it is generally the base for the European national seismic zonations. Ground motions expected in and around Tbilisi are between 0.16 and 0.24 g and higher values, between 0.24 and 0.32 g, are forecasted in the proximity of some faults present in the neighbourhood of Tbilisi. The highest ground motions, *PGAs* larger than 0.56 g, refer to the Caucasus structures, in the northern part of the map, while values between 0.48 and 0.56 g refer to the Javakheti area, in the south-western part of the map.

Similar features can be seen also in the map for a stiff soil (Fig. 10b) with increased values. *PGAs* between 0.24 and 0.32 g can be seen now around Tbilisi, between 0.56 and 0.64 g in the Javakheti area, and larger than 0.64 g for the Caucasus structures.

The differences shown by the soft soil map (Fig. 10c) with respect to the stiff soil map are marginal: a stronger ground motion (larger than 0.72 g) is expected along the Caucasus structures and slightly lower *PGAs* are forecasted in the Javakheti area.

As the modern seismic zonations (see e.g.: Frankel *et al.,* 2002; Adams and Halchuk, 2003) consider also the 2475-year return period (2% exceedence probability in 50 years) as standard reference, this additional return period has been used for the computation of the seismic hazard maps of eastern Georgia. The 3 maps in Figs. 10d, 10e, and 10f show similar features to the previous maps but the expected values are remarkably higher. The Tbilisi area remains below 0.56 g also in the case of poor soil conditions (Fig. 10e and 10f) while *PGAs* larger than 1.12 are expected on the rocks of the Caucasus (Fig. 10d). *PGAs* larger than 0.80 and 1.12 g are forecasted in the Javakheti area, on rock (Fig. 10d) and poor soil (Figs. 10e and 10f), respectively.

9. The soil seismic hazard map of the Tbilisi broader area

The Tbilisi broader area (see its limits in Fig. 1) was considered for a more detailed analysis. Several geological and geotechnical maps, prepared during the Soviet period (Institute of Geology of Georgia, Caucasus Institute of Mineralogy), and borehole data, taken from the database of the Georgian State Oil Company "Saqnavti", were used to classify the different soils. In addition, the map of the Quaternary deposits in the Tbilisi broader area, showing the deposit thicknesses, was used to delineate the different terrains on the basis of the types of deposits (proluvial, alluvial, etc.). The types of outcropping rocks and those of rocks beneath the deposits were also specified on the basis of the geological maps. The average velocity of the S waves in the upper 30 m (V_{30}) was estimated mainly from the borehole stratigraphic profiles, and was assigned to each terrain. At the final stage, V_{30} was assigned to each point of a grid covering the study area with a 200-m spacing and the different terrains, previously identified, were classified according to the NEHRP provisions (BSSC, 1997). More precisely, 5 soil types have been considered: hard rock (NEHRP class A), rock (class B), soft rock (class C), stiff soil (class D), and soft soil (class E). These classes correspond to specific V_{30} intervals: $V_{30} \geq 1500$ m/s, $1500 > V_{30} \geq 760$, $760 > V_{30} \geq 360$, $360 > V_{30} \geq 180$, $V_{30} < 180$ m/s. Tbilisi town is characterized by all three kinds of rock, while stiff soil can be found only SE of the town (Fig. 11a). The European seismic code (CEN, 2002) considers only 4 soil classes: rock, stiff soil, soft soil, and very soft soil. Also these classes are based on the V_{30} value. Comparing the NEHRP classes to the EC8
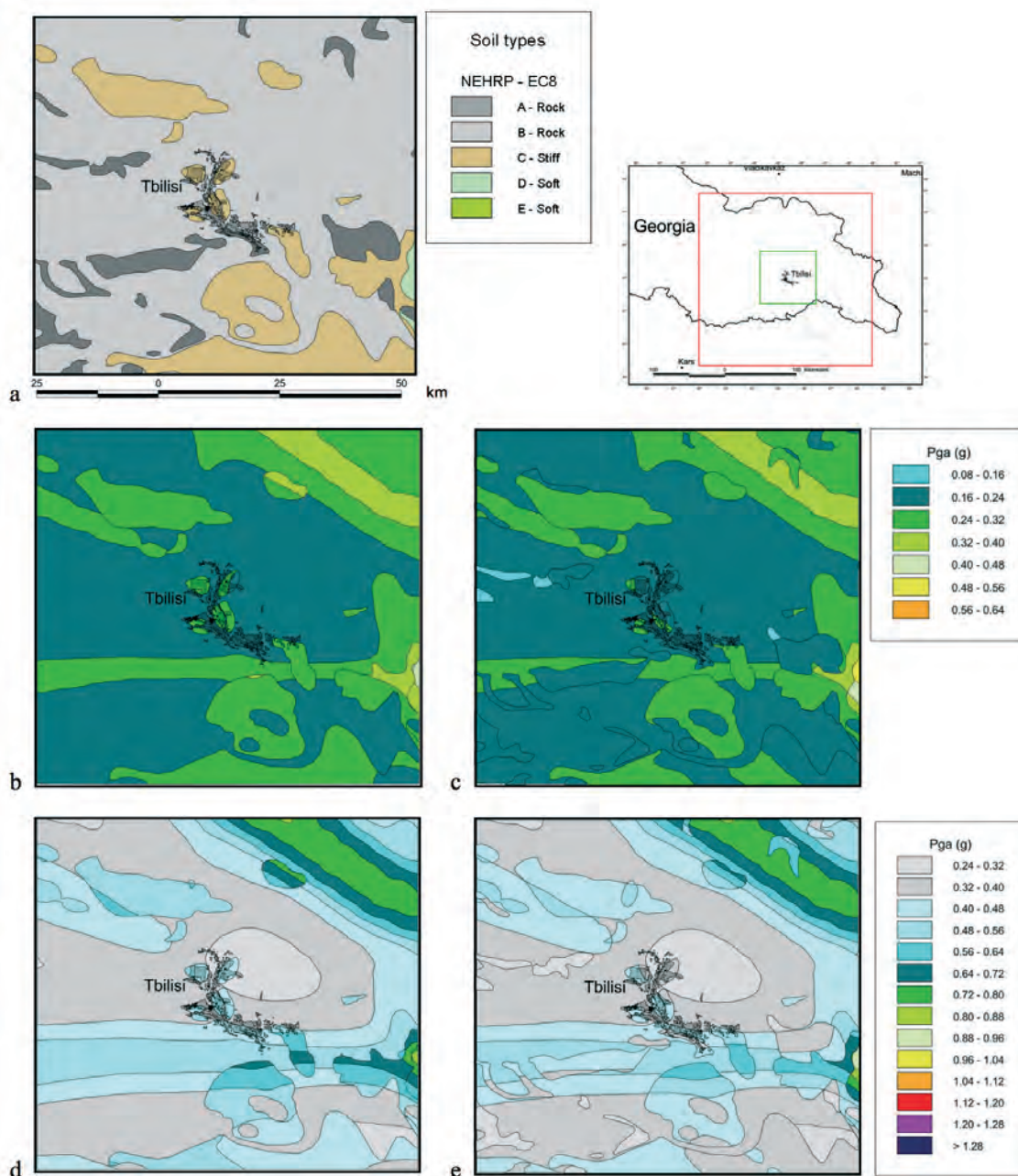
Fig. 11 – Soil types and soil seismic hazard in the Tbilisi broader area. Soil types (a) according to the NEHRP provisions (BSSC, 1997) and the EC8 seismic code (CEC, 2000); the *PGA* computed taking into account the attenuation variability: for a 475-year return period according to soil-dependent ARs (b), and according to the NEHRP amplification factors (c); for a 2475-year return period according to soil-dependent ARs (d), and according to the NEHRP amplification factors (e).
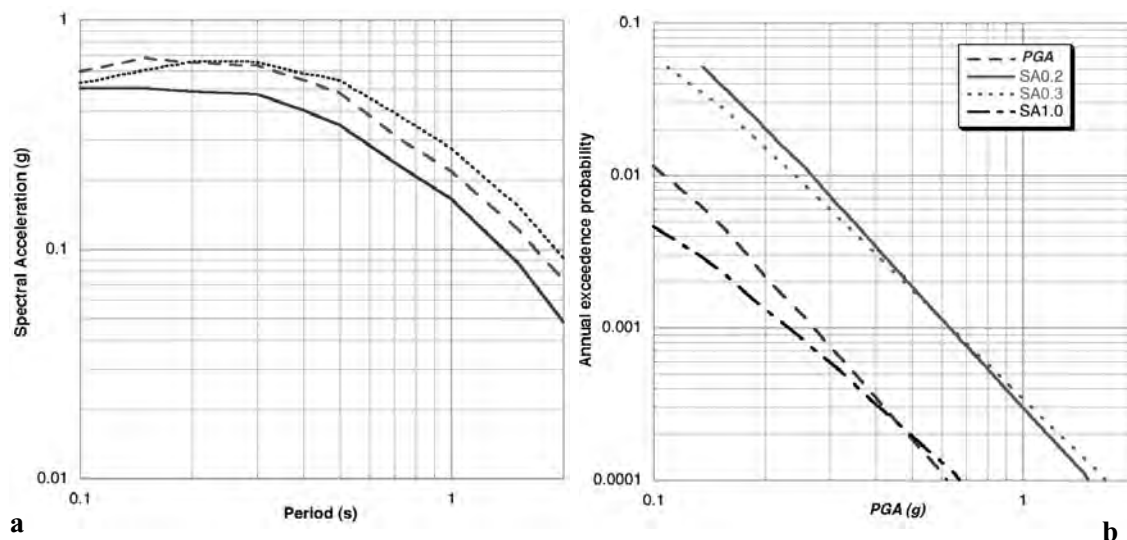
Fig. 12 – Seismic hazard in Tbilisi: a) uniform hazard response spectrum for 3 soil types: rock (solid line), stiff soil (dashed line), and soft soil (dotted line); b) hazard curve for *PGA* (dashed line), *SA0.2* (solid line), *SA0.3* (dotted line), and *SA1.0* (dash-dotted line).

ones, it can be roughly established that the EC8 rock class corresponds to the A plus B NEHRP classes, EC8 stiff soil corresponds to NEHRP class C, EC8 soft soil to NEHRP class D, and EC8 very soft soil to NEHRP class E. The AMB soil-dependent AR does not separate soft soil from very soft soil because of the scarcity of data referring to those classes in the European strong motion data bank (Ambraseys *et al.,* 2000, 2004). Fig. 11a can be viewed, then, in a simplified way where only 3 EC8 classes are defined: rock, stiff soil, and soft soil.

Taking into account the EC8 soil typologies identified in the study region (Fig. 11a), the adequate *PGA* value of the regional maps (Fig. 10) has been associated to the different area units using the potentialities of a GIS and the final EC8 soil hazard maps have been constructed (Figs. 11b, and 11d). Moreover, the NEHRP (BSSC, 1997) amplification factors (0.8 for soil type A, 1.0 for type B, 1.2 for type C, and 1.5 for type D) have been applied to the rock hazard maps (Figs. 10a and 10d) and the final NEHRP soil hazard maps have been obtained (Figs. 11c and 11e). The EC8 map referring to the 475-year return period (Fig. 11b) shows that in Tbilisi town *PGAs* between 0.16 and 0.32 g are expected according to the soil conditions. Larger ground motions (between 0.32 and 0.40 g) are forecasted for the sector of the study region which is closest to the Caucasus ridge and is located about 40 km NE of Tbilisi, while the maximum *PGAs* computed (values larger than 0.40 g) refer to the Gareji Semi-desert area, which is situated about 30 km ESE of the town and is characterized by a highly eroded soil. Similar features can be seen on the map obtained by applying the NEHRP amplification factors (Fig. 11c): Tbilisi is characterized by the same *PGAs* while slightly higher values can be found in the area situated about 40 km ESE of the town (values larger than 0.48 g). A much more complex situation is displayed by the map referring to the 2475-year return period (Figs. 11d and 11e). In this case, *PGAs* between 0.24 and 0.64 g are expected for the different districts of Tbilisi according to their

different soil conditions for the EC8 map (Fig. 11d). For the NEHRP map (Fig. 11e), conversely, the maximum *PGA* remains below 0.56 g. Again to the NE of the town, the area with high seismic hazard (*PGAs* larger than 0.72 g in both maps) can be seen, while to the ESE values larger than 0.88 g are forecasted by the NEHRP map.

It is well known that *PGA* is a poor quantity to describe seismic hazard because it is a specific characteristic of the ground motion time history that does not necessarily represent the main feature of the record, for example *PGA* can be related to a single spike with high frequency contents which is not dangerous to buildings. For this reason, the seismic hazard of Tbilisi has been computed also in terms of uniform hazard response spectrum for the 3 soil types of the EC8 building code (Fig. 12a). In this case, only the AMB AR has been considered because the S+S one is defined for the *PGA* only. As expected, the rock response spectrum is characterized by lower values of the spectral ordinates than those referring to soil. The intersection around 0.2 s between the stiff and the soft soil spectra is worth noting: for short periods the stiff soil spectrum is higher than the soft soil one while for periods larger than 0.3 s the soft soil spectrum dominates.

Fig. 12b represents the global seismic hazard of Tbilisi because the complete hazard curve is reported for *PGA* and 3 spectral accelerations (*SAs*) summarizing the contents of the response spectrum at 0.2 s (*SA0.2*), 0.3 s (*SA0.3*), and 1.0 s (*SA1.0*).

10. Conclusions

A complete seismic hazard analysis has been performed for eastern Georgia with specific attention to the Tbilisi broader area. The contents of the earthquake catalogue have been revised and updated and a new *PGA* AR for the Caucasus has been established. Different hypotheses about the seismogenesis, the M_{max}, and the attenuation model have been taken into account by the use of the logic tree approach (Fig. 2). Seismic hazard maps referring to three soil types and to the 475- and 2475-year return periods have been computed for eastern Georgia (Fig. 10). They show that the highest *PGAs*, between 0.56 and 0.64 g on rock for the 475-year return period, are expected along some faults of the Caucasus, while ground motions exceeding 0.64 g can occur on soil in the Javakheti area, always for the 475-year return period.

A more detailed analysis has interested the Tbilisi broader area because a map of the soil typologies existing in the region has been prepared on geological basis (Fig. 11a). The soil seismic hazard maps have been constructed by associating, with the help of the GIS facilities, the ground motion related to the specific terrains. For the 475-year return period, *PGAs* between 0.16 and 0.32 g are expected according to the soil conditions in Tbilisi town (Figs. 11b and 11c), while values between 0.24 and 0.56 g are forecasted for a 2475-year return period (Figs. 11d and 11e). The uniform hazard response spectrum for Tbilisi (Fig. 12a) pinpoints the expected building response. It is almost flat for periods lower than 0.3 s for rock and stiff soil and decreases for higher periods. The decrease is less evident for soft soil and the spectrum remains high for periods lower than 0.5 s.

thanks are due to an anonymous reviewer, who formulated fruitful remarks.

REFERENCES

Adams J. and Halchuk S.; 2003: *Fourth generation seismic hazard maps of Canada: values for over 650 Canadian localities intended for the 2005 National Building Code of Canada.* Open File 4459, Geological Survey of Canada, Ottawa, 155 pp.

Albarello D., Bosi, V., Bramerini F., Lucantoni A., Naso G., Peruzza L., Rebez A., Sabetta F. and Slejko D.; 2000: *Carte di pericolosità sismica del territorio nazionale.* Quaderni di Geofisica, 12 Editrice compositori, Bologna, 7 pp.

Albarello D. and Mucciarelli M.; 2002: *Seismic hazard estimates using ill-defined macroseismic data at site.* Pure Appl.Geophys., **159**, 1289-1304.

Ambraseys N.N.; 1990: *Uniform magnitude re-evaluation of European earthquakes associated with strong-motion records.* Earthq. Eng. struct. Dyn., **19**, 1-20.

Ambraseys N.N., Simpson K.A. and Bommer J.J.; 1996: *Prediction of horizontal response spectra in Europe.* Earth. Eng. Struct. Dyn., **25**, 371-400.

Ambraseys N., Smit P., Berardi R., Rinaldis D., Cotton F. and Berge C.; 2000: *European strong-motion database.* Imp. College - ENEA - IPSN - Servizio Sismico - Sogin, London, CD-Rom.

Ambraseys N., Douglas J., Sigbjornsson R., Berge-Thierry C., Suhadolc P., Costa G. and Smit P.; 2004: *European strong-motion database Volume 2.* Imp. College – Earthq. Eng. Res. Center - IRSN – Univ. Trieste, London, CD-Rom.

Balassanian S., Ashirov T., Chelidze T., Gassanov A., Kondorskaya N., Molchan G., Pustovitenko B., Trifonov V., Ulomov V., Giardini D., Erdik M., Ghafory-Ashtiany M., Gruenthal G., Mayer-Rosa D., Schenk V. and Stucchi M.; 1999: *Seismic hazard assessment for the Caucasus test area.* Annali di Geofisica, **42**, 1139-1151.

Barani S., Spallarossa D., Bazzurro P., Eva C.; 2007: *Sensitivity analysis of seismic hazard for Western Liguria (North Western Italy): a first attempt towards the understanding and quantification of hazard uncertainty.* Tectonophysics, **435**, 13–35.

Bender B. and Perkins D.M.; 1987: *Seisrisk III: a computer program for seismic hazard estimation.* U.S. Geological Survey Bulletin 1772, 48 pp.

Bius Ye.I.; 1948: *Seismic Conditions of the Trans-Caucasus, Part I.* Acad. Sci. U.S.S.R., Tbilisi.

Bius Ye.I.; 1952: S*eismic Conditions of the Trans-Caucasus, Part II.* Acad. Sci. U.S.S.R., Tbilisi.

Bius Ye.I.; 1955: *Seismic Conditions of the Trans-Caucasus, Part III.* Acad. Sci. U.S.S.R., Tbilisi.

Bragato, P.L.; 2004: *Regression analysis with truncated samples and its application to ground-motion attenuation studies.* Bull. Seism. Soc. Am., **94**, 1369-1378.

Bragato P.L. and Slejko D.; 2005: *Empirical ground motion attenuation relations for the eastern Alps in the magnitude range 2.5-6.3.* Bull. Seism. Soc. Am.*,* **95**, 252-276.

BSSC (Building Seismic Safety Council); 1997: *NEHRP recommended provisions for seismic regulations for new buildings.* Part 1 - Provisions, 1997 edition. BSSC, Washington D.C., 337 pp.

Camassi R. and Stucchi M.; 1997: *NT4.1, a parametric catalogue of damaging earthquakes in the Italian area (release NT4.1.1).* GNDT, Milano, 66+XXVII pp.

CEN (Comité Européen de Normalisation); 2002: *Eurocode 8: design of structures for earthquake resistance. Part 1: general rules, seismic actions and rules for buildings.* Draft No 5, Doc CEN/T250/SC8/N317, CEN, Brussels, 100 pp.

Coppersmith K.J. and Youngs R.R.; 1986: *Capturing uncertainty in probabilistic seismic hazard assessments within intraplate environments.* In: Proceedings of the Third U.S. National Conference on Earthquake Engineering, August 24-28, 1986, Charleston, SC, Earthquake Engineering Research Institute, El Cerrito CA U.S.A., vol. 1, pp. 301-312.

Cornell, C.A.; 1968: *Engineering seismic risk analysis.* Bull. Seism. Soc. Am., **58**, 1583-1606.

Frankel A.D., Petersen M.D. Mueller C.S., Haller K.M., Wheeler R.L., Leyendecker E.V., Wesson R.L., Harmsen S.C., Cramer C.H., Perkins D.M. and Rukstales K.S.; 2002: *Documentation for the 2002 update of the national seismic hazard maps.* Open-File Report 02-420, U.S. Geological Survey, Denver, 33 pp.

Gamkrelidze I., Giorgobiani T., Kuloshvili S., Lobjanidze G. and Shengelaia G.; 1998: *Active deep faults map and the catalogue for the territory of Georgia.* Bull. Georgian Ac. Sciences, **157**, 80-85.

Giardini D.; 1999: *The Global Seismic Hazard Assessment Program (GSHAP) - 1992/1999.* Annali di Geofisica, **42**, 957-974.

Giardini D. and Basham P.(eds); 1993: *Global Seismic Hazard Assessment Program.* Annali di Geofisica, **33**, n. 3 - 4.

Gruppo di Lavoro; 2004: *Redazione della mappa di pericolosità sismica prevista dall'Ordinanza PCM del 20 marzo 2003.* Rapporto conclusivo per il Dipartimento della Protezione Civile, INGV, Milano – Roma, 65 pp. + 5 App.

Jackson, J.A.; 1992: *Partitioning of strike-slip and convergent motion between Eurasia and Arabia in eastern Turkey and the Caucasus.* J. Geoph. Res., **97**, 12,471-12,479.

Kijko A. and Graham G.; 1998: *Parametric-historic procedure for probabilistic seismic hazard analysis. Part I: estimation of maximum regional magnitude mmax.* Pure Appl. Geophys., **152**, 413-442.

Kondorskaya N.V. and Shebalin N.V.; 1982: *New catalogue of the strong earthquakes of the USSR from ancient times through 1977.* Report SE-31, World Data Center-A for Solid Earth Geophysics, Boulder, Colorado U.S.A., 608 pp.

Kulkarni R.B., Youngs R.R. and Coppersmith K.J.; 1984: *Assessment of confidence intervals for results of seismic hazard analysis.* In: Proceedings of the Eighth World Conference on Earthquake Engineering, July 21-28, 1984, San Francisco CA U.S.A., Prentice-Hall Inc., Englewood Cliffs NJ U.S.A., vol. 1, pp. 263-270.

Mark R.K.; 1977: *Application of linear statistical model of earthquake magnitude versus fault length in estimating maximum expectable earthquakes.* Geology, **5**, 464-466.

Martirosyan A., Balassanian S., Simonian R. and Asatryan L.; 1999: *Computation of probabilistic seismic hazard for the GSHAP test area 'Caucasus'.* Natural Hazards, **20**, 1-20.

McGuire R.K.; 1977: *Seismic design spectra and mapping procedures using hazard analysis based directly on oscillator response.* Earthq. Engin. Struct. Dyn., **5**, 211-234.

McGuire R.K.; 2001: *Deterministic vs. probabilistic earthquake hazards and risks.* Soil Dynamics and Earthquake Engineering, **21**, 377-384.

McGuire R.K. and Shedlock K.M.; 1981: *Statistical uncertainties in seismic hazard evaluations in the United States.* Bull. Seism. Soc. Am., **71**, 1287-1308.

Philip H., Cisternas A., Gvishiani A. and Gorshkov A.; 1989: *The Caucasus: an actual example of the intial stages of continental collision.* Tectonophysics, **161**, 1–21.

Rautian T.G., Khalturin V.I., Fujita K., Mackey K.G. and Kendall A.D.; 2007: *Origins and methodology of the Russian energy K-class system and its relationship to magnitude scales.* Seismol. Res. Lett., **78**, 579-590.

Rebez A. and Slejko D.; 2004: *Introducing epistemic uncertainties into seismic hazard assessment for the broader Vittorio Veneto area (N.E. Italy).* Boll. Geof. Teor. Appl., **45**, 305-320.

Shebalin N.V. and Tatevossian R.E.; 1997: *Catalogue of strong earthquakes (M >6.0) for the global seismic hazard assessment program: test area of Caucasus.* In: Giardini D. and Balassanian S. (eds), Historical and prehistorical earthquakes in the Caucasus, NATO ASI Series, Kluwer Academic pub., pp. 1-32.

Slejko D., Peruzza L. and Rebez A.; 1998: *Seismic hazard maps of Italy.* Annali di Geofisica, **41**, 183-214.

Smit P., Arzoumanian V., Javakhishvili Z., Arefiev S., Mayer-Rosa D., Balassanian S. and Chelidze T.; 2000: *The digital accelerograph network in the Caucasus area.* In: Balassanian S. (ed), Earthquake hazard and seismic risk reduction - Advances in natural and technological hazard research, Kluwer Ac. Publ., Dordrecht.

Stepp J.C.; 1972: *Analysis of completeness of the earthquake sample in the Puget Sound area and its effect on statistical estimates of earthquake hazard.* In: Proceedings of First Int. Conference on Microzonazion, Seattle Washington, vol. 2, pp. 897-910.

Toro G.R., Abrahamson N.A. and Schneider J.F.; 1997: *Model of strong motions from earthquakes in central and eastern North America: best estimates and uncertainties.* Seism. Res. Lett., **68**, 41-57.

Triep E.G., Abers G.A., Lerner-Lam A.L., Mishatkin V., Zakharchenko N. and Starovoit O.; 1995: *Active thrust front of the Greater Caucasus: the April 29, 1991, Racha earthquake sequence and its tectonic implications.* J. Geoph. Res., B, **100**, 4011–4033.

Varazanashvili O. and Papalasvili V.; 1998: *Reconstruction of strong earthquake parameters by historical data of XI-XIV centuries.* Journal of Georgian Geophysical Society, **3**, 77-84.

Wells D.L. and Coppersmith K.J.; 1994: *New empirical relationship among magnitude, rupture length, rupture width, rupture area, and surface displacement.* Bull. Seism. Soc. Am., **84**, 974-1002.

Corresponding author: Dario Slejko
Istituto Nazionale di Oceanografia e di Geofisica Sperimentale
Borgo Grotta Gigante 42c, 34010 Sgonico (Trieste), Italy
phone: +39 040 2140248; fax: +39 040 327307; e-mail: dslejko@ogs.trieste.it